

Diffractive structure functions in nuclei

T. Lappi^{1,2}, H. Kowalski³, C. Marquet^{2,4} and R. Venugopalan⁵

1- Department of Physics P.O. Box 35, 40014 University of Jyväskylä, Finland

2- Institut de Physique Théorique, CEA/DSM/Saclay, 91191 Gif-sur-Yvette, France

3- Deutsches Elektronen-Synchrotron DESY, 22607 Hamburg, Germany

4- Department of Physics, Columbia University, New York, NY 10027, USA

5- Physics Department, Brookhaven National Laboratory, Upton, NY 11973, USA

We calculate proton and nuclear diffractive structure functions in the IPsat (Kowalski-Teaney) dipole model. This parametrization has previously been shown to provide good agreement with inclusive F_2 measurements and exclusive vector meson measurements at HERA. We discuss how the impact parameter dependence crucially affects our analysis, in particular for small β .

1 Introduction

The large fraction of diffractive events observed at HERA shows that modern colliders are approaching the nonlinear regime of QCD, where gluon saturation and unitarization effects become important. In Deep Inelastic Scattering (DIS) on nuclei the nonlinear effects are enhanced by the possibility of interacting coherently with several nucleons simultaneously [2]. There are plans for several facilities capable of high energy nuclear DIS experiments, as the EIC [3] and LHeC [4] colliders. Due to the difficulty in measuring an intact recoil nucleus deflected by a small angle, diffractive eA collisions present an experimental challenge. But if they are successful, nuclear diffractive DIS (DDIS) would provide a good test of our understanding of high energy QCD.

In the high energy limit DIS is best understood in the dipole frame, where the incoming virtual photon fluctuates into a quark-antiquark pair which then interacts with the target. The scattering amplitude is related to the correlator of two Wilson lines in the wavefunction of the nucleus. In contrast to the language of collinearly factorized parton distribution functions, in this formalism both inclusive and diffractive observables can be calculated from the same universal dipole cross section. This enables one to naturally use the dipole cross sections fitted to one process to predict observables in another one. In this talk we will review the results of our recent work [5] to apply this ideology to computing nuclear diffractive structure functions. Our emphasis is not on the most recent developments of high energy evolution equations, but the effects of a more realistic and consistent impact parameter dependence. This will lead us to discuss, in addition to the consequences of nuclear geometry on diffractive observables, the importance of the proton impact parameter profile used in the calculations. In this paper we shall first describe the dipole cross sections and calculation methods used and then summarize our results for nuclear DDIS.

2 Method

We decompose the diffractive structure function into different components in the standard way as

$$x_{\mathbb{P}} F_2^{\text{D}}(x_{\mathbb{P}}, \beta, Q^2) = x_{\mathbb{P}} F_{T,q\bar{q}}^{\text{D}}(x_{\mathbb{P}}, \beta, Q^2) + x_{\mathbb{P}} F_{L,q\bar{q}}^{\text{D}}(x_{\mathbb{P}}, \beta, Q^2) + x_{\mathbb{P}} F_{T,q\bar{q}g}^{\text{D}}(x_{\mathbb{P}}, \beta, Q^2). \quad (1)$$

For the lowest Fock state of the virtual photon wavefunction, the $q\bar{q}$ dipole ($F_{T,q\bar{q}}^D$ and $F_{L,q\bar{q}}^D$) we follow the treatment of [6]. At small β (large mass of the diffractive system) the dominant contribution comes from higher Fock states. In this work we are interested in the finite experimentally relevant range of \sqrt{s} and will only include the leading (in α_s) $q\bar{q}g$ -component of these. In different works this component has been evaluated in different limits, we shall here use the approach of [7] and interpolate between the small β , large N_c formula used in [8] and the finite β , large Q^2 form used in [6]. We refer the reader to the references above for the detailed formulae.

We use the “IPsat” dipole cross section parametrization introduced in Ref. [9] and extensively studied in Ref. [10]. This is an impact parameter dependent dipole cross section that combines unitarization and the correct behavior of structure functions the logarithmic large Q^2 (i.e. small dipole size r) behavior of structure functions are achieved. This is achieved using an eikonalized DGLAP-evolved gluon distribution function [11]. The dipole cross section is given by

$$\frac{d\sigma_{\text{dip}}}{d^2\mathbf{b}_T} = 2 \left[1 - \exp(-r^2 F(x, r) T(\mathbf{b}_T)) \right], \quad (2)$$

where F is proportional to the DGLAP evolved gluon distribution

$$F(x, r^2) = \frac{\pi^2}{2N_c} \alpha_s(\mu^2(r^2)) xg(x, \mu^2(r^2)), \quad (3)$$

with both the coupling and the gluon distribution $xg(x, Q^2)$ evaluated at the scale $\mu^2(r^2) = \mu_0^2 + C/r^2$.

Several works on the subject (e.g. [12, 6, 13, 14]) assume, explicitly or implicitly, a factorizable \mathbf{b}_T dependence of the dipole cross section.

$$\frac{d\sigma_{\text{dip}}}{d^2\mathbf{b}_T}(\mathbf{b}_T, \mathbf{r}_T, x) \sim e^{-\frac{b_T^2}{2B}}, \quad (4)$$

which leads to an exactly exponential t -dependence of diffractive cross sections. The conceptual problem with the form Eq. (4) is that it cannot be a solution of the BK equation (unless the profile is a θ function, which would contradict the experimentally observed t -distribution). A factorized Gaussian profile for the proton dipole cross section, for example, *does not approach the correct unitarity limit* for $b \neq 0$. This is the main motivation for including the impact parameter dependence in the saturation scale model (2), not as a factorizable prefactor of the dipole cross section. For a proton the impact parameter profile in Eq. (2) is taken as $T(\mathbf{b}_T) = T_p(\mathbf{b}_T) \sim \exp(-\frac{b^2}{2B_G})$ and for a nucleus $T(\mathbf{b}_T) = \sum_{i=1}^A T_p(\mathbf{b}_T - \mathbf{b}_{T_i})$, where the nucleon coordinates \mathbf{b}_{T_i} are taken from a standard Woods-Saxon distribution [15]. The concrete consequence of this impact parameter dependence is that, in contrast to the factorized ansatz (4), the different components of

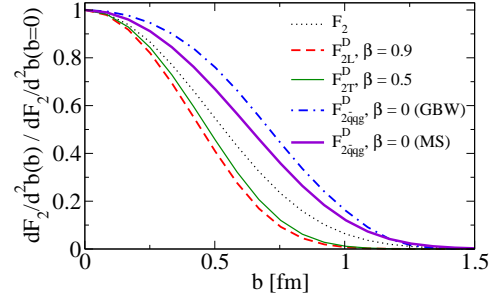


Figure 1: Contributions of different impact parameters to the inclusive and diffractive structure functions in the proton in the IPsat model.

the saturation scale model (2), not as a factorizable prefactor of the dipole cross section. For a proton the impact parameter profile in Eq. (2) is taken as $T(\mathbf{b}_T) = T_p(\mathbf{b}_T) \sim \exp(-\frac{b^2}{2B_G})$ and for a nucleus $T(\mathbf{b}_T) = \sum_{i=1}^A T_p(\mathbf{b}_T - \mathbf{b}_{T_i})$, where the nucleon coordinates \mathbf{b}_{T_i} are taken from a standard Woods-Saxon distribution [15]. The concrete consequence of this impact parameter dependence is that, in contrast to the factorized ansatz (4), the different components of

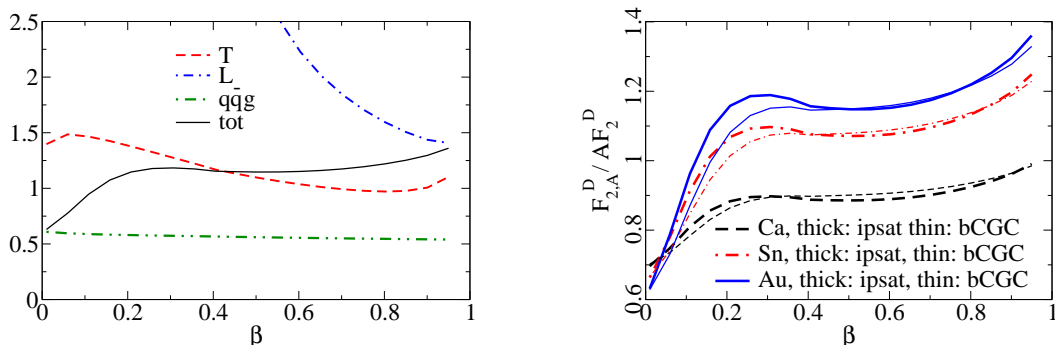


Figure 2: Left: dependence on β of nuclear effects on the individual components of the diffractive structure function in a gold nucleus. Right: total β -dependence of nuclear effects on the diffractive structure function. In both plots $Q^2 = 5 \text{ GeV}^2$ and $x_{\mathbb{P}} = 10^{-3}$.

the diffractive structure have different b -dependences from each other and from the inclusive cross section. The $q\bar{q}$ -component is enhanced at small b (closer to the black disk limit), whereas the $q\bar{q}g$ -part is dominated by larger b (because it vanishes in the black disk limit). This structure is illustrated in Fig. 1.

3 Results

3.1 HERA

We compare our calculation to the HERA results on diffractive structure functions, measured using both using the rapidity gap method (ZEUS FPC [16] and H1 LRG [17]) and by measuring the recoil proton (ZEUS LPS [18] and H1 FPS [19]). Because the FPC and LRG data include events in which the proton has broken up, the cross-sections measured for the process $ep \rightarrow eXY$ are larger than the one measured for the process $ep \rightarrow eXp$. We scale down this data by a constant factor to correct for the proton dissociation contribution; the ZEUS FPC data by a factor of 1.45 and the H1 LRG data by 1.23. These factors are different due to the different cuts on M_Y , the mass of the proton dissociation system. For the combined dataset from ZEUS and H1 data both with and without identified protons we get $\chi^2/N_{\text{dof}} = 1.3$, with a coefficient $\alpha_s = 0.14$ of the $q\bar{q}g$ term. This is the values of α_s that we shall use to evaluate nuclear diffractive structure functions in the next section. For the IPsat model the largest contribution to the χ^2 comes from the rapidity gap method data at large β . The fit to only the LPS ($\chi^2 = 0.5$ IPsat) and FPS ($\chi^2 = 0.8$) is much better. Considering just the LPS also accommodates a larger value of $\alpha_s = 0.21$ with still $\chi^2 < 1$.

The fit to HERA data is better with a smaller α_s than in Ref. [7]. Given the b -dependence described previously this is to be expected. The factorized b -dependence used in earlier calculations of the diffractive structure function such as Refs. [6, 7] forces the $q\bar{q}g$ -component to have the same impact parameter dependence as the $q\bar{q}$ -component. As discussed above, the $q\bar{q}g$ component is sensitive to larger impact parameters and is thus larger; in order to fit the same data this must be compensated by multiplying it with a smaller factor of α_s .

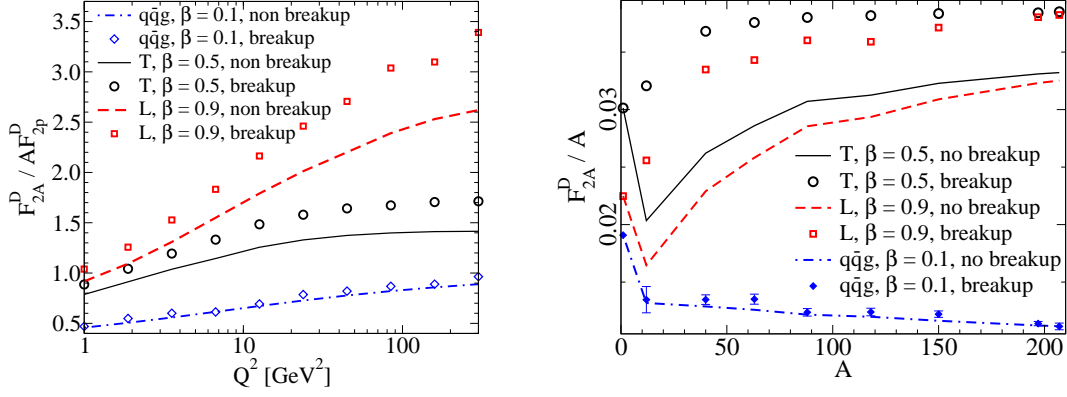


Figure 3: Left: dependence of the gold diffractive structure function on Q^2 . Right: dependence of the nuclear diffractive structure function on the mass number A for $Q^2 = 5 \text{ GeV}^2$. In both plots $x_{\mathbb{P}} = 10^{-3}$.

3.2 Predictions for nuclei

In Fig. 2 we show the ratios of different components of the gold diffractive structure function to the proton one as a function of β . The $q\bar{q}$ -components of the F_{2A}^D are enhanced compared to A times the proton diffractive structure functions. This is to be expected, because of the fact that in a gold nucleus the dipole cross section is, on average over the transverse area, closer to the unitarity limit than the proton - it is “blackier”. The elastic scattering probability of a $q\bar{q}$ dipole is maximal in the “black disk” limit and the approach to it is quicker in a large nucleus. The $q\bar{q}g$ component, on the other hand, is suppressed for nuclei compared to the proton. This is due to the fact that in a nucleus the scattering amplitude is closer to the unitarity limit, when the $q\bar{q}g$ component vanishes. This leads to a nuclear suppression of the diffractive structure function in the small β region, where the $q\bar{q}g$ component dominates. The net result of the different contributions is that F_{2A}^D , for a large range in β , is close to AF_{2p}^D . In Fig. 2, we plot the total ratio as a function of β for different nuclei in the “non breakup” case. As expected from our prior discussion, one sees a strong enhancement with A for larger β and likewise, a stronger suppression with A at very small values of β .

In our formalism, if one requires that the nucleus stays completely intact, the average over the nucleon positions \mathbf{b}_{Ti} must be performed at the amplitude level. This is the case of *coherent* diffraction. If the nucleus is allowed to break up into color neutral constituents (referred to as *incoherent* diffraction), the average is performed at the level of the cross section. Measuring the intact recoil nucleus at such a small t experimentally at a future electron ion collider is challenging, so it is useful to consider both cases. A comparison of the “breakup” versus “non breakup” cross-sections can be seen in the left panel of Fig. 3 for the ratio of diffractive cross-sections as a function of Q^2 . The results in Fig. 3 for the ratio of diffractive structure functions indicate that the diffractive cross-section in nuclei decrease more slowly for large Q^2 than in the proton. This can be understood as a consequence of Q_s being larger for nuclei and diffraction being much more sensitive to Q^2/Q_s^2 than inclusive DIS. In the right panel of Fig. 3, the nuclear size A dependence of the longitudinal and transverse components of the diffractive structure function is shown for the “breakup” and

“non breakup” cases. In the “breakup” case, one sees a very weak A dependence. In the coherent “non breakup” case, one first notes that the diffractive structure function first decreases up to atomic numbers $A \sim 10$, before beginning to rise. As noted in Ref. [2], this is due to the typical scattering amplitude for small nuclei actually being smaller than for a proton because of the diluteness of the nucleus. This leads to a suppression of coherent diffraction. The “breakup” case, on the other hand, can only be enhanced in nuclei. For gold nuclei, the cross sections in the “non breakup” case are about 15% lower than in the “breakup” case.

Because of the different nuclear modifications in inclusive and diffractive scattering, the fraction of diffractive events in an experiment depends on the detailed kinematics and experimental coverage. For moderate values of Q^2 and large nuclei we expect a nuclear shadowing of the inclusive structure function by a factor ~ 0.8 [2]. A typical nuclear enhancement of diffraction (at moderate values of $\beta \gtrsim 0.2$) is a factor of ~ 1.2 . Combining these we expect $\sigma_D/\sigma_{\text{tot}}$ to be increased by a factor of $1.2/0.8 = 1.5$ compared to the proton. Thus from a typical ep fraction of 15% we expect $\sigma_D/\sigma_{\text{tot}}$ to go up to 20% – 25% at an eA collider.

Acknowledgments

T. Lappi is supported by the Academy of Finland, project 126604. RV’s research is supported by DOE Contract No. DE-AC02-98CH10886. CM’s research is supported by the European Commission under the FP6 program, contract No. MOIF-CT-2006-039860.

References

- [1] <http://indico.cern.ch/contributionDisplay.py?contribId=105&sessionId=26&confId=53294>.
- [2] H. Kowalski, T. Lappi and R. Venugopalan, Phys. Rev. Lett. **100**, 022303 (2008), [arXiv:0705.3047 [hep-ph]].
- [3] A. Deshpande, R. Milner, R. Venugopalan and W. Vogelsang, Ann. Rev. Nucl. Part. Sci. **55**, 165 (2005), [arXiv:hep-ph/0506148].
- [4] J. B. Dainton, M. Klein, P. Newman, E. Perez and F. Willeke, JINST **1**, P10001 (2006), [arXiv:hep-ex/0603016].
- [5] H. Kowalski, T. Lappi, C. Marquet and R. Venugopalan, Phys. Rev. **C78**, 045201 (2008), [arXiv:0805.4071 [hep-ph]].
- [6] K. J. Golec-Biernat and M. Wusthoff, Phys. Rev. **D60**, 114023 (1999), [arXiv:hep-ph/9903358].
- [7] C. Marquet, Phys. Rev. **D76**, 094017 (2007), [arXiv:0706.2682 [hep-ph]].
- [8] S. Munier and A. Shoshi, Phys. Rev. **D69**, 074022 (2004), [arXiv:hep-ph/0312022].
- [9] H. Kowalski and D. Teaney, Phys. Rev. **D68**, 114005 (2003), [arXiv:hep-ph/0304189].
- [10] H. Kowalski, L. Motyka and G. Watt, Phys. Rev. **D74**, 074016 (2006), [arXiv:hep-ph/0606272].
- [11] J. Bartels, K. J. Golec-Biernat and H. Kowalski, Phys. Rev. **D66**, 014001 (2002), [arXiv:hep-ph/0203258].
- [12] K. J. Golec-Biernat and M. Wusthoff, Phys. Rev. **D59**, 014017 (1999), [arXiv:hep-ph/9807513].
- [13] E. Iancu, K. Itakura and S. Munier, Phys. Lett. **B590**, 199 (2004), [arXiv:hep-ph/0310338].
- [14] M. S. Kugeratski, V. P. Goncalves and F. S. Navarra, Eur. Phys. J. **C46**, 413 (2006), [arXiv:hep-ph/0511224].
- [15] C. W. De Jager, H. De Vries and C. De Vries, Atom. Data Nucl. Data Tabl. **36**, 495 (1987).
- [16] ZEUS, S. Chekanov *et al.*, Nucl. Phys. **B713**, 3 (2005), [arXiv:hep-ex/0501060].
- [17] H1, A. Aktas *et al.*, Eur. Phys. J. **C48**, 715 (2006), [arXiv:hep-ex/0606004].
- [18] ZEUS, S. Chekanov *et al.*, Eur. Phys. J. **C38**, 43 (2004), [arXiv:hep-ex/0408009].
- [19] H1, A. Aktas *et al.*, Eur. Phys. J. **C48**, 749 (2006), [arXiv:hep-ex/0606003].